

GEORGALLI, G. A., EKSTEEN, J. J., BEZUIDENHOUT, R., VAN BEEK, B. and GOFF, T. Towards electrode immersion control on Lonmin's No. 1 circular furnace. *Third International Platinum Conference 'Platinum in Transformation'*, The Southern African Institute of Mining and Metallurgy, 2008.

Towards electrode immersion control on Lonmin's No. 1 circular furnace

G. A. GEORGALLI*, J. J. EKSTEEN†, R. BEZUIDENHOUT†, B. VAN BEEK† and T. GOFF†

*University of Stellenbosch, South Africa

†Lonmin, South Africa

A control philosophy to be applied by Lonmin to maintain constant electrode immersion in their No. 1 circular smelting furnace is put forward. This control philosophy is facilitated through a combination of thermodynamic models used to predict the slag composition and empirical correlations to estimate the furnace geometric factor as well as the slag conductivity. The model can determine the operating resistance setpoint required in order to maintain a desired electrode immersion as a function of the feeds to the furnace, slag level and temperature. If modifying the resistance setpoint cannot maintain the desired immersion without moving out of the furnace P-V-I operating envelope, the model can be used to determine the amount of slag modifiers (silica or lime) required to shift the slag chemistry back into a region where the immersion can be controlled through resistance setpoint manipulation.

Introduction

Lonmin treats a wide variety of concentrates and recycled materials (reverts, dusts, slag mill concentrates, etc.) in its smelting furnaces. This leads to a variable feed composition that influences the conductivity/resistivity of the slag melts obtained. Historically, Lonmin made use of XRF to obtain the total elemental chemistry of the furnace feed. However, the association of particularly iron with oxygen, silica, chromium and sulphur in its various oxide, sulphide, chromite, and silicate forms posed a convoluted problem that could not be simplified without additional analysis, particularly to make a split in oxidic iron and sulphidic iron. The oxidic iron contributes to the slag phase while sulphidic iron contributes to matte fall. A highly variable matte fall in itself is highly problematic as matte may build up above the slag tap line, and lead to explosion hazards during slag granulation. Moreover, a rapidly increasing matte fall causes problems with ladle logistics when ladles are rotated between the furnaces and the Peirce-Smith Converters.

In recent research¹ it was shown that the conductivity of melter slags in the PGM industry is the most sensitive to the amounts of ferrous iron and silica in slags, as well as the slag temperature. Ferrous iron shows strong electronic conduction, over and above ionic conduction that is the normal conduction mechanism for ions in molten slags, leading to a very large increase in conductivity with increase in concentration. Conversely, silica, because of its tendency to form large polymerised cations, contributes the most to the resistive behaviour of slags, inhibiting the transport of cations through the molten silicate medium. Chromium (as Cr₂O₃) is noted to play an insignificant role in slag resistivity. However, this does not imply that chromium-rich concentrates have little effect on slag conductivity. On the contrary, UG2 concentrates are significantly richer in FeO-type iron than Merensky based concentrates. Superimposed on this is the large amount of

ferrous and ferric iron re-entering the furnaces via slag mill concentrates, especially where these concentrates are derived from converter slag rich in fayalite, magnetite and other iron-based spinels. The control of lime addition (which further increases slag conductivity) is also crucial as it may exacerbate the effects of FeO, if already present in larger-than-normal concentrations.

This high variability in the FeO:SiO₂ ratio in slags has significant risks if the resistance setpoint is not adjusted to make up for the change in resistivity. This is particularly of importance in melter furnaces with such high hearth power densities as found in Lonmin circular No. 1 furnace. If a resistance setpoint is maintained constant, but the feed mix to the furnace leads to slags of increasing FeO:SiO₂ ratio and consequently high conductivities, the electrode immersion decreases to increase the current path length and the associated contribution of the geometric factor. This leads to poorer stirring and PGM recovery, more Cr-spinel settling, and increased probability of sintering in the concentrate bed. Conversely, if the FeO:SiO₂ ratio decreases significantly, the conductivity decreases, forcing the electrodes down to still maintain the resistance setpoint (assuming it has not changed). This may bring the electrode tips dangerously close to the matte, leading to matte overheating, and the risk of burn-through of the hearth, or matte run-outs, both having catastrophic impacts on production and very large safety hazards.

Ideally, the control philosophy should cater for maintaining a constant immersion in the melt (the required immersion is dependent on what is optimal with regards to PGM recovery to matte while still maintaining the required smelting rate). In such a case, the resistance setpoint has to be adjusted to compensate for changes in slag chemistry, temperature and variable slag levels. Empirical on-plant measurements (electrode immersion and dip tests), in conjunction with recent research on the relationship between slag resistivity and slag chemistry for platinum

melter slags, have made it possible to establish reliable models to relate the operating resistance, the furnace geometric factor (a function of electrode immersion, slag depth and the cell constant of the furnace) and the slag resistivity (function of chemistry and temperature). With these relationships established, and if the feed to the furnace is well characterised, thermodynamic models can be added to predict the slag composition based on the furnace feed and slag temperature. This then allows for the operating resistance setpoint changes required for constant electrode immersion to be determined in a feedforward manner.

Control philosophy

Lonmin is now in process to establish a laboratory to perform mineralogical characterization of furnace feed in conjunction with chemical (XRF) analysis. The mineralogical analysis, once reconciled with the chemical analysis, will provide a basis for the estimation of the split between oxidic and sulphidic iron in the feed. This information is used, in a cascade control philosophy, together with measured slag chemistry, slag levels and temperature, to estimate future slag chemistries and associated slag conductivity. These variables are therefore the disturbance variables in the control system. This information is subsequently used to calculate the conductivity and geometric factor, using % immersion as setpoint. The manipulated variable then becomes the resistance (impedance) setpoint. As the resistance setpoint changes, the current re-establishes at a new equilibrium value, based on a fixed power setting (which in turn is linked to the tons of concentrate smelted), according to:

$$I = \sqrt{\frac{P}{R \cdot PF}} \quad [1]$$

For a realistic control system, the P-V-I behaviour has to fall within the obtainable P-V-I operating envelope of the furnace, and the available transformer taps. The only way to handle excessively conductive slags while still maintaining a reasonable immersion is via minor SiO₂ addition; conversely, excessively resistive slags require minor amounts of lime addition to maintain a required immersion while staying within the P-V-I envelope. The addition of slag modifiers (SiO₂/CaO fluxes) is dependent on whether the required immersion can be obtained within the constraints of the P-V-I envelope. One also needs to be cognisant of the effects of slag chemistry modification on slag viscosity. To perform feedforward prediction of the matte fall, the FeO/FeS split, etc., the equilibrium slag/matte chemistry is predicted using FactSage software, which also predicts the slag and matte chemistries. Various feed mineralogy and chemistries are evaluated using FactSage to build up a sufficiently large database of input-equilibrium output combinations. This input-output dataset is then used to train a multilayer perceptron, back propagation neural network, comprehensively validated and tested on unseen datasets. Once the trained network predicts the outcomes with sufficient accuracy, the network structure is encoded in the decision support algorithm used to predict slag and matte levels and chemistries and phase relationships. The cascade arrangement, which measures current chemistries using a combination of XRF and XRD, temperatures and levels are then used in combination with the predicted feed chemistries and feed rates to estimate

future slag chemistries and slag and matte levels and the associated conductivities, geometric factors and the resistance value required to obtain the required immersion.

Modelling methodology

Before the models and correlations used to facilitate electrode immersion control are described in detail, it is convenient to review the overall modelling philosophy as alluded to in the previous sections.

The slag conductivity and furnace operating resistance setpoint are linked through the furnace geometric factor (f_g) as shown in Equation [2]:

$$R = \frac{f_g}{\sigma} \quad [2]$$

where R is the resistance and σ is the slag conductivity.

The furnace geometric factor is a function of the furnace geometry, electrode diameters, and electrode immersion and is estimated empirically by conducting dip tests on the furnace in question. For a particular furnace only the electrode immersion can be changed, as the furnace geometry and electrode diameter are constants. Thus, if the slag composition and its resulting conductivity can be predicted, and the furnace geometric factor accurately estimated, the resistance setpoint that is required in order to achieve the desired immersion can be calculated.

Key to this approach is the thermodynamic model used to predict the slag chemistry. This model was created using the FactSage thermodynamic software package and neural networks. Thermodynamic software packages are extremely useful and powerful but they are difficult to use within control systems due to the obvious problems of creating an interface between such a modelling package and a control system. The creators of these packages are, however, aware of this problem and there are tools on the market which allow these packages to be used within control systems (e.g. ChemApp). However these systems still suffer from the problem that they use Gibbs Free Energy minimization to determine the composition and amounts of the relevant phases. Using a minimization routine within a control system gives rise to an entirely new set of problems. Iterative minimization routines take time to solve which can cause lags in the control system but more critically, one can be guaranteed that sooner or later the minimization routine will hang. For obvious reasons this is extremely undesirable and can cause operational as well as safety issues.

Thus a modelling methodology is required that can utilize the power of the thermodynamic software packages in a fast and robust manner. This was achieved by generating data using FactSage and then modelling these data using neural networks^{2,3}. Neural networks are essentially non-linear regression equations. Just as for linear regression equations, parameters are estimated by minimizing the difference between the predicted output (from the regression equation) and the data being used to estimate the parameters. Neural networks are very good for modelling non-linear data and especially so if the data contain no noise, as is the case for the data generated using FactSage. Thus, training a neural network on the generated FactSage data allows one to access the information derived from FactSage in a quick, accurate and robust manner that can be used within a control system.

Neural networks do, however, have their own pitfalls.

While they are excellent at interpolation this does not guarantee that they can extrapolate and they must therefore always be used within the ranges of the data used to train them. Thus great care was taken when deciding upon the ranges of the input variables used when running the simulations in FactSage which make up the database used to train the neural networks.

Creation of the thermodynamic database

As was discussed in the previous section, neural network models cannot be expected to extrapolate outside of the range of the data that they were trained on. Deciding upon the ranges to be used for the FactSage simulations and the sampling resolution within those ranges is a balancing act. On the one hand, the ranges must be large enough to ensure that the neural network trained on the generated data is never required to extrapolate. Having a large range is, however, not sufficient as if the sampling within that range is done at too low a resolution there is a chance that some effects within the system may be missed and the interpolation of the neural network may be incorrect. On top of all this is the computational (especially with regard to memory) restrictions on the amount of data that one can use to train neural networks (especially when they have many inputs and outputs). Thus, the selection of this range is of critical importance and requires a good understanding of the feeds to the furnace at that moment and in the future. On the other hand, changes in the mine plan and thus the concentrate smelted in the No. 1 furnace must be accounted for or the models will cease to be valid.

Determining the ranges used in FactSage simulations

In order to meet the requirements described above, a normal probability density function (PDF) was created for each input variable except silica, lime and the temperature, all of which were given uniform distributions. This was done to ensure that the database used to train the neural networks had the highest resolution in the area where it would normally be expected to operate, but also sufficient resolution in the less probable operating regions so that the neural network will not need to extrapolate into regions where it was not trained.

Lonmin commissioned full chemical and mineralogical analyses of the primary and secondary concentrate streams entering the smelter as well as the smelter recycle streams⁴. This information, along with the Lonmin dry concentrate delivery plan⁵ up to and including 2013 was used to determine the ranges of the input variables used in the FactSage simulations. The inputs used in the FactSage simulations were Ni, Cu, Fe, S, FeO, Al₂O₃, MgO, Cr₂O₃, CaO, SiO₂ and C (from the electrode consumption) as well as the temperature. All of the inputs to FactSage (except iron) were expressed in the same way that they are when the feed is analysed using XRF (as is done at the smelter). This is an acceptable manner to proceed when doing thermodynamic simulations as long as one does not want to do an energy balance. As can be seen, iron was input as Fe and FeO, the portion of the iron feed which was expressed in elemental form was that which is associated with sulphide minerals such as chalcopyrite, pyrite, pentlandite, etc. Once the feed to the furnace is subject to XRD analysis it will be possible to calculate the split between iron entering the furnace as a sulphide (FeS) and that entering as an oxide (FeO). All of the feeds were varied for the simulations except the carbon from the electrode

consumption, which was taken as a constant. Ingress air was not included as a feed. Although the ingress air is a source of oxygen to the furnace, the amount of oxygen entering through this medium is considered negligible when compared to the oxygen that enters the furnace through the oxides in the feed, which is substantial.

The compositions and magnitudes of the main streams (concentrates), secondary streams (slag float) and reverts (crushed converter slag, crushed furnace bricks, and crushed refractories) were used to determine the average values for the input feed variables. These average values were then used as the mean for probability density functions (PDFs) that were created for each input variable. The standard deviation to be used in each PDF was chosen by looking at compositions of the main and secondary streams only (concentrates and slag plant float) as these were the major contributors to the furnace feed. The standard deviation for each PDF was chosen in such a manner that the extreme values found in some of the main and secondary streams would correspond to the values obtained for the 99% and 1% probability of the PDF. By determining the ranges in this manner, it is ensured that the resolution of the FactSage simulations is highest for the most probable compositions of the feed to the furnace while at the same time managing to ensure that the less probable feed compositions are still simulated and thus the neural network is not ever going to be required to extrapolate. Thus two important criteria are met and the number of FactSage simulations required does not become ridiculous.

Silica, lime and the temperature were the only variables where normal PDFs were not applied. The temperature distribution was uniform between 1 500 and 1 750°C. For lime, a uniform distribution between 1 and 11 wt % was used. The silica for each simulation was then set to be equal to 100 minus all of the other compositional inputs, so that the compositional inputs into FactSage were always normalised to 100%. The data were then filtered to ensure that only silica values between 30 and 55 wt % were used in the simulations.

FactSage simulations

In total, 77 298 simulations were done in FactSage. Of these, 50 000 were used as training data, 5 000 as validation data during training in order to ensure that the networks did not overfit the data, and the final 22 298 were used to test the networks once they had been trained. The following solution models were used when doing the simulations in FactSage:

- Liquid solutions: FTmisc-MATT (matte), FToxid-SLAGA (slag)
- Solid solutions: FToxid-SPIN (spinel), FToxid-oPyr (orthopyroxene), FToxid-Oliv (olivine)
- Gas: Gas ideal.

The FactSage output is in the form of a text file and, as such, extraction of the relevant data can be rather tedious, especially when working with such a large number of simulations. While normally the required data can be exported directly to an Excel spreadsheet from FactSage, this becomes impossible when working with more than 65 536 rows of data, as this is the row limit within an Excel spreadsheet. The export function within FactSage is also sometimes unstable and relatively time-consuming when working with large amounts of data. Thus the post-processing was done using PHP scripting language and Matlab.

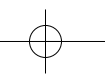


Table I
Neural network properties

	Bulk slag	Liquid slag	% Solids + MF
Input nodes	11	11	11
Output Node	9	10	2
Hidden layers	1	1	1
Nodes in hidden layer	20	20	10
Transfer function		Tanh	
Net training function		Bayesian regulation backpropagation	
Performance function		Mean squared error	
Wight/bias learning function		Gradient descent with momentum	

Table II
Neural network model performance on testing data

Bulk slag			Liquid slag			% Solids + MF		
Output	R ² (%)	MSE (wt %)	Output	R ² (%)	MSE (wt %)	Output	R ² (%)	MSE (wt %)
Fe ²⁺	99.43	6.5×10^{-5}	FeO	99.78	0.102	% Solids	98.42	0.032
FeO	99.87	0.159	Fe ₂ O ₃	99.35	0.003	Matte fall	99.96	0.016
CaO	99.96	0.100	Al ₂ O ₃	99.61	0.081			
MgO	99.94	0.072	CaO	99.94	0.125			
SiO ₂	99.96	0.066	MgO	99.81	0.220			
Al ₂ O ₃	99.74	0.062	CrO	98.73	0.053			
Cr ₂ O ₃	99.63	0.017	Cr ₂ O ₃	97.78	0.025			
Cu ₂ O	99.09	8.4×10^{-4}	SiO ₂	99.85	0.044			
NiO	99.26	9.7×10^{-4}	Cu ₂ O	98.93	0.002			
			Slag total	99.56	1.243			

Neural network models

All of the neural networks were trained using Matlab 7.5.0. Due to memory limitations, all of the outputs required for this project could not be modelled using one neural network. In total three neural networks were trained:

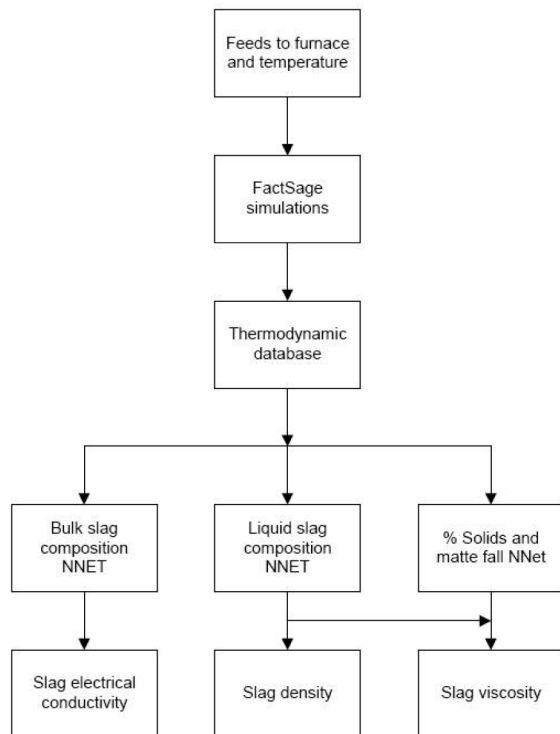


Figure 1. Diagram describing the modelling methodology used

- **Bulk slag composition.** This is the slag composition including both the liquid portion of the slag and all of the solids (spinel, orthopyroxene and olivine) and represented as if the slag were analysed using an XRF as is done on the smelter. The Fe²⁺ ratio is also modelled in the neural network and it is the bulk composition from this neural network that is used to calculate the slag conductivity using the model of Hundermark¹.
- **Liquid slag composition.** This neural network models the composition of the liquid slag only. This network is used to determine the liquid portion of the slag viscosity as well as the slag density.
- **Percentage solids and matte fall.** This network models the percentage solids in the slag as well as the matte fall.

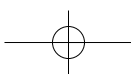
The manner in which each of the developed neural networks was used within the greater model is shown in Figure 1. The bulk slag neural network is used only to determine the slag conductivity. The liquid slag neural network is used to determine both the slag viscosity and density. From the third network, the percentage solids is used only to determine the slag viscosity.

The properties of the three neural networks are given in Table I. All of the neural networks trained have the same inputs, namely (and in order): temperature, Ni, Cu, Fe, S, Al₂O₃, Cr₂O₃, MgO, FeO, CaO and SiO₂, where the temperature is in °C and the compositional inputs in wt % (normalized to 100%).

The performance of the neural networks on the testing data is shown in Table X. It is clear that the networks model the FactSage output very well, which is to be expected as the data are generated and therefore contain no noise.

Furnace geometric factor model

On 9 November 2007, a dip test was done by Lonmin personnel and the researcher on the Lonmin No. 1 furnace.



The aim of this test was to generate a curve of the electrode resistance vs electrode immersion, which can then be used to estimate the cell constant for the furnace geometric factor model. While there have been many furnace geometric factor models published in the literature, with the most recent being that of Jiao and Themelis⁶, the majority of these models were calibrated on cold systems in the lab and at power fluxes well below those found in modern industrial furnaces. Sheng *et al.*⁷ compared the results from some of these correlations to industrial data from a 6-in-line nickel smelting furnace and found that they severely underestimated the resistance (which is related to the furnace geometric factor and slag conductivity through Equation [2]). Thus, in order to use a geometric factor correlation with confidence, it must be calibrated on the furnace in question by performing dip tests.

While the model used cannot be shown here due to confidentiality, it essentially has the following form:

$$f_g = f(k, X_s, H_s, D_e) \quad [3]$$

Where k is the cell constant, H_s is the slag height, X_s the penetration of the electrode into the slag and D_e the electrode diameter (as shown in Figure 2). Equation [2] relates the furnace geometric factor to the resistance and the slag conductivity. Thus, the resistance vs electrode immersion curve obtained from the dip test can be used to estimate the cell constant k as long as the slag composition and temperature are known, as these are used to determine the slag conductivity using the correlation of Hundermark¹ as shown in Equation [4].

Two values for k were regressed from the dip test data, one where all the data were used (Figure 3(a)) and one where the low immersion data (< 10%) were excluded (Figure 3(b)). What is apparent from Figure 3 is the slight decrease in model performance when including the low immersion data.

As the immersion approaches zero, the resistance increases exponentially and is asymptotic with the y-axis, thus small measurement errors are compounded at low immersions resulting in significant scatter in the data. As the furnace is hardly operated at immersions lower than

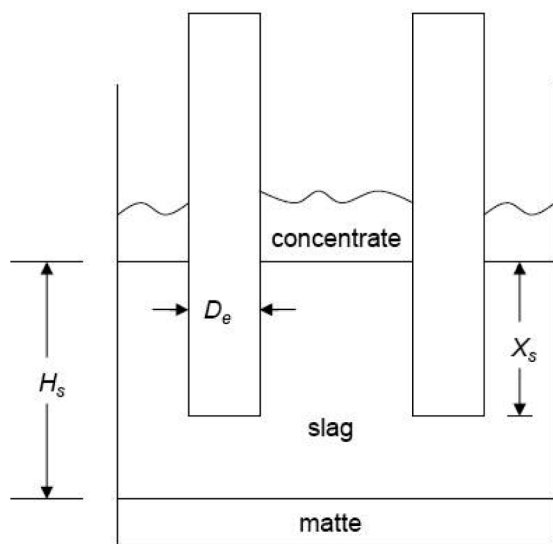


Figure 2. Illustration of the geometric variables used in the empirical model for the determination of the furnace geometric factor

10%, it was felt that including these data would be counterproductive when using the geometric factor model in the normal operating regime. It is considered more important to have a correlation which functions more accurately within the range of normal furnace operation than one which sacrifices performance in this range in order to be more general. The k values regressed with all of the data will, however, not be discarded and should a need arise to run the furnace with immersions less than 15%, this k value can be used.

Slag physical property models

Using the outputs from the different neural networks, the physical properties of the slag (viscosity, density, and electrical conductivity) were calculated. In this way the effect of the composition of the feed to the furnace on such factors as tapping, mixing and refractory wear can be assessed in a feed forward manner.

The slag conductivity is determined using the correlation of Hundermark¹ that was developed specifically for PGM smelting slags. The model uses the bulk slag composition as input, i.e. the overall composition of the slag that is a combination of the liquid and solid phases present in the slag. All elements are expressed in their most probable form (i.e. Al as Al_2O_3 , Fe as FeO, etc.), as is done when a slag is analysed using XRF on the smelter. The only extra terms added to the correlation are the fractions of the iron in the slag which are in the ferric and ferrous form. As such, the output from the bulk slag composition neural network is used as input to the model of Hundermark to determine the slag conductivity.

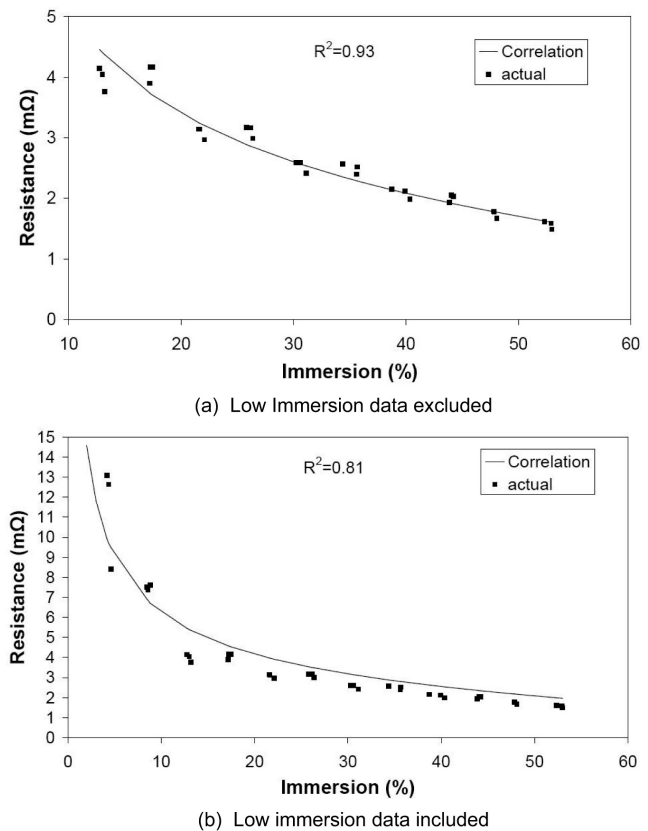


Figure 3. Line plots of actual resistance vs predicted resistance for dip test

$$\begin{aligned} \ln \sigma = & \left(19.9 - \frac{47\,348}{T}\right) \cdot X_{\text{Al}_2\text{O}_3} + \left(15.4 - \frac{24\,087}{T}\right) \cdot X_{\text{CaO}} \\ & + \left(9.2 - \frac{14\,151}{T}\right) \cdot X_{\text{MgO}} + \left(-0.5 - \frac{7\,478}{T}\right) \cdot X_{\text{SiO}_2} \\ & + \left(10 - \frac{9\,140}{T}\right) \cdot X_{\text{FeO}} \cdot \text{Fe}^{2+} + \left(65.4 - \frac{82\,447}{T}\right) \\ & \cdot X_{\text{FeO}}^2 \cdot \text{Fe}^{2+} \cdot \text{Fe}^{3+} + \left(-2.6 + \frac{6\,642}{T}\right) \cdot X_{\text{FeO}} \cdot \text{Fe}^{3+} \end{aligned} \quad [4]$$

Where T is the slag temperature in K, X is the mol fraction of the components and Fe^{2+} and Fe^{3+} are the fractions of ferrous and ferric ions respectively.

The sensitivity of the conductivity on selected slag components is shown in Figure 4. This was done by taking a typical slag composition at 1 600°C and then perturbing each variable by 10% in both a positive and negative direction. As the components are present in different amounts in the slag, the data were then normalized to be percentage change in the relevant component. In this way, a realistic representation of the effect of the different components is obtained. From the sensitivity analysis it is clear that an increase in FeO, CaO or MgO increases the slag conductivity while an increase in Al_2O_3 and SiO_2 decreases it. The slag density and viscosity were calculated using the correlations of Utigard and Warczok⁸. They reviewed both density and viscosity data for copper/nickel sulphide smelting and converting slags from various publications and fitted correlations to the published data. For both the slag density and viscosity, the compositional variables are those of the liquid portion of the slag only and as such the liquid slag composition neural network outputs are used as inputs to these correlations.

The liquid slag density is calculated using the following equation;

$$\rho = 5 - 0.03(\text{SiO}_2 + \text{Fe}_2\text{O}_3) - 0.02(\text{CaO} + \text{MgO}) + \text{Al}_2\text{O}_3 + \text{Na}_2\text{O} + 0.035 \cdot \text{Cr}_2\text{O}_3 - 0.001(T - 1\,473) \quad [5]$$

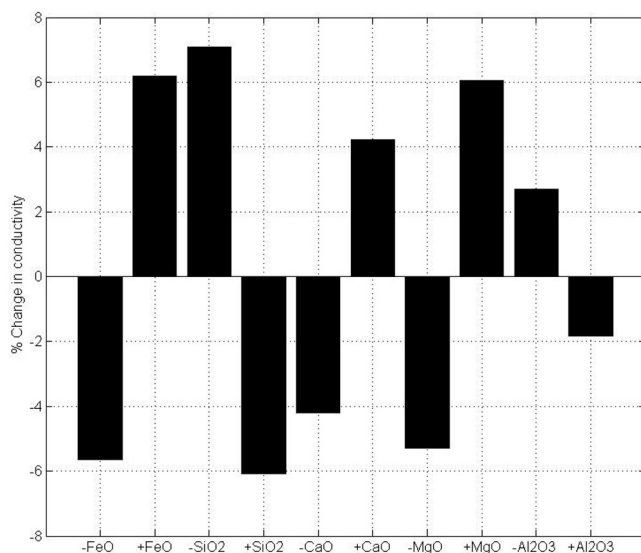


Figure 4. Sensitivity analysis for selected slag components at 1 600°C using the model of Hundermark¹

where the density is in g/cm^3 , the slag temperature in K and the components in wt %. The density given by Equation [5] is that of the liquid portion of the slag only.

The viscosity of the slag is made up of two parts. Firstly, the viscosity of the liquid portion of the slag, which is determined using the Equations [6] through [9]⁸:

$$\log \eta_0 = -0.49 - 5.1VR^{0.5} + \frac{-3\,660 + 12\,080VR^{0.5}}{T} \quad [6]$$

$$VR = \frac{A}{B} \quad [7]$$

$$A = \text{SiO}_2 + 1.5\text{Cr}_2\text{O}_3 + 1.2\text{ZrO}_2 + 1.8\text{Al}_2\text{O}_3 \quad [8]$$

$$B = 1.2\text{FeO} + 0.5(\text{Fe}_2\text{O}_3 + \text{PbO}) + 0.8\text{MgO} + 0.7\text{CaO} + 2.3(\text{Na}_2\text{O} + \text{K}_2\text{O}) + 0.7\text{Cu}_2\text{O} + 1.6\text{CaF}_2 \quad [9]$$

where the temperature is in K and the composition in wt %. This is, however, not sufficient as there are more often than not solid particles in the slag, which have a large effect on the slag viscosity. The viscosity of the slags with solids can be represented by the Einstein-Roscoe equation in the form given by Zhang *et al.*⁹ up to 33 mass % solids:

$$\eta = \eta_0 (1 - af)^{-n} \quad [10]$$

where η and η_0 are the viscosity of the solid-containing and solid-free melt, respectively. The parameters a and n are constants, while f is the mass fraction of solids in the melt. The value of the constants a and n is dependant on the particle size of the solids within the melt. The values used by Zhang *et al.*⁹ ($a = 3.0$ and $n = 2.5$) were determined for spinel particles, which are the predominant solid particles in Cu/Ni smelting slags.

Results

Effect of slag modifiers

A typical feed composition and a slag temperature of 1 600°C were used as inputs to the neural networks to assess the effect of the slag modifiers. The same inputs were also fed into FactSage so that the results using the outputs from the neural networks could be compared to those using the outputs from FactSage. The effect of CaO on the slag conductivity, viscosity of the liquid portion of the slag, bulk slag viscosity and the fraction of chrome in the feed dissolved in the liquid slag is shown in Figure 5.

From Figure 5 it is clear that lime addition increases the conductivity of the slag while lowering the viscosity of both the liquid portion and the bulk slag. Lime addition also decreases the solubility of chrome in the slag. While the decrease in slag viscosity is without doubt advantageous, the effects of lime addition on the slag conductivity and solubility of chrome in the liquid slag are definitely not.

Similar plots for silica content in the feed are shown in Figure 6. In all cases, silica has the opposite effect to lime. From Figures 5 and 6, it is clear that the results using the outputs from the neural networks compare extremely well to those using the outputs from FactSage.

The effect of the slag modifiers (CaO and SiO_2) on the liquid slag viscosity was shown in Figures 5(b) and 6(b). The viscosity of the liquid portion of the slag has a great effect on the operation of the furnace as the matte droplets that form in the slag must settle through the slag layer. Similarly, any solid particles in the slag, such as spinel

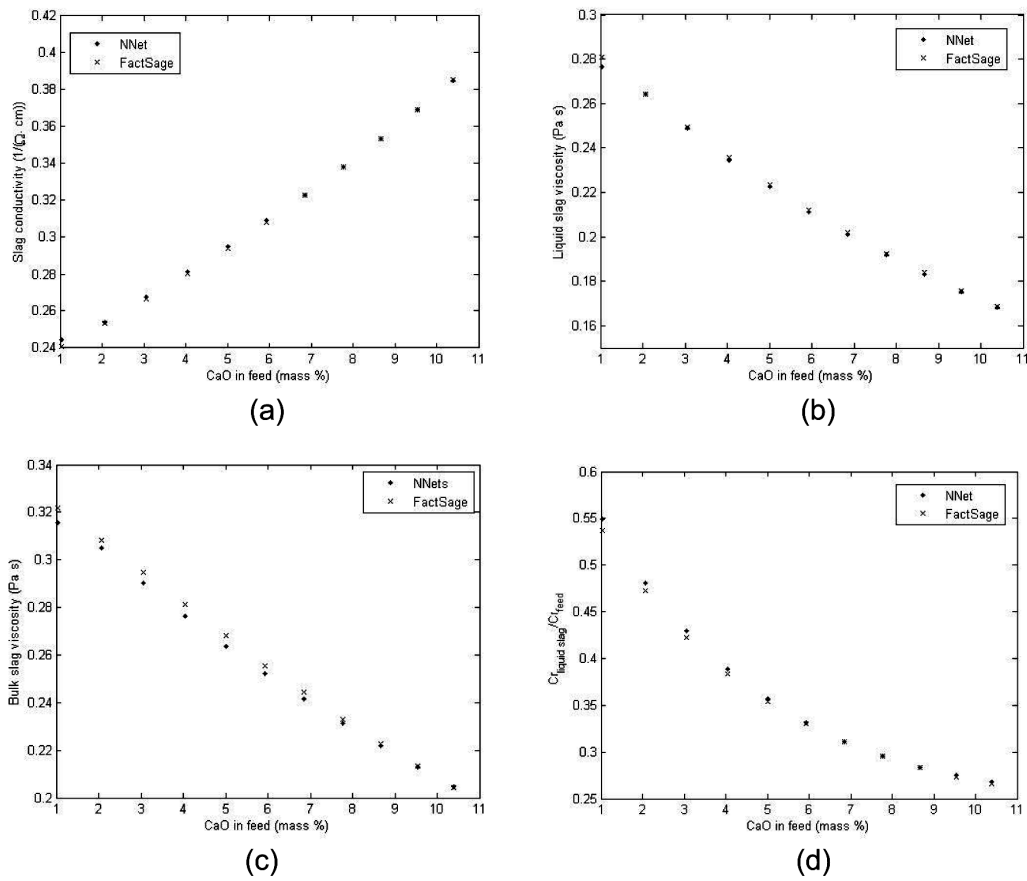


Figure 5. Effect of lime addition on (a) slag electrical conductivity, (b) viscosity of the liquid portion of the slag, (c) bulk slag viscosity, (d) fraction of chrome in feed dissolved in liquid slag

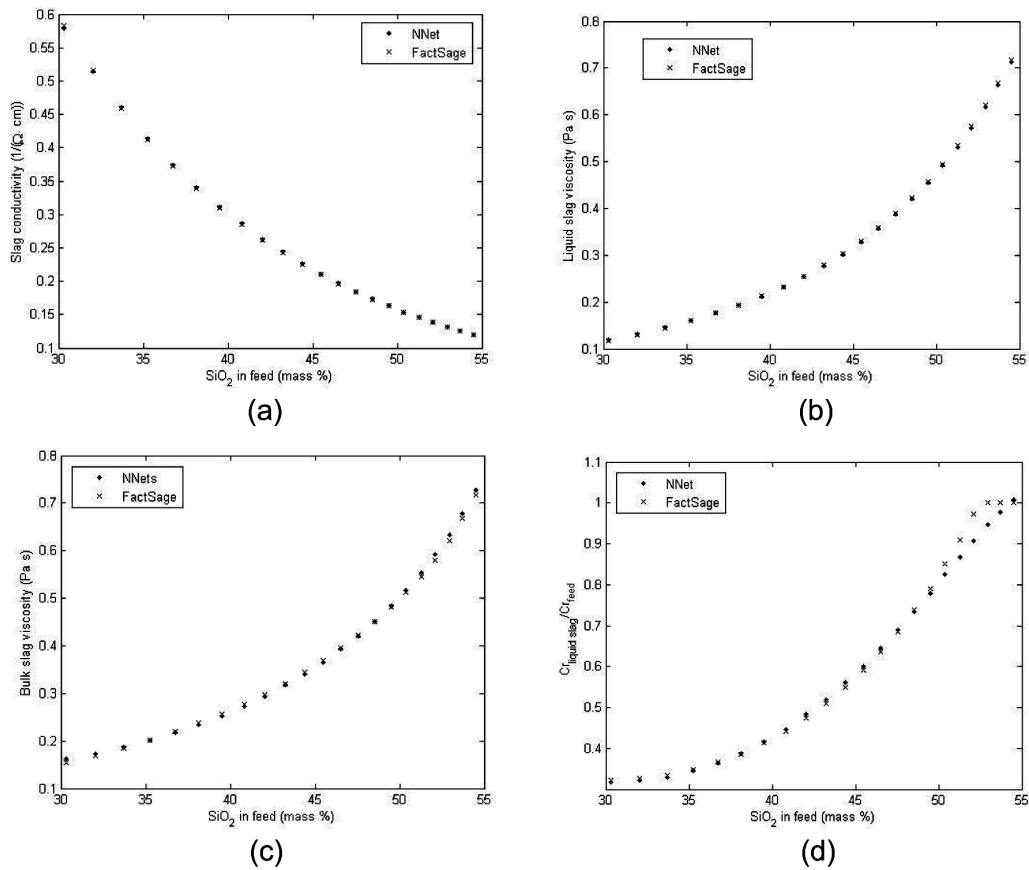


Figure 6. Effect of silica addition on (a) slag electrical conductivity, (b) viscosity of the liquid portion of the slag, (c) bulk slag viscosity, (d) fraction of chrome in feed dissolved in liquid slag

crystals, will also settle through the slag and due to their density, which is between that of the slag and matte, probably settle at the matte slag interface. A simple calculation was done in order to assess the effect of the liquid slag viscosity on the settling rate of the matte droplets or spinel crystals. The terminal velocity of the droplets or particles in the slag was calculated using Stokes law¹⁰:

$$V_T = \frac{D^2 \cdot g(\rho_{\text{particle}} - \rho_{\text{fluid}})}{18\eta_0} \quad [11]$$

Where ρ_{particle} is the density of the particle/droplet which is settling in the slag, ρ_{fluid} is the density of the slag (calculated using Equation [5]), η_0 is the viscosity of the liquid portion of the slag (calculated using Equations [6] through [9]), D is the diameter of the particle/droplet and g is the acceleration due to gravity. If we assume the spinel and matte density as 4 500 and 55 00 kg/m³ respectively and take the slag level as 1 m (an average value obtained from Lonmin), the time taken for the droplet/particle to settle through the slag can be calculated. This was done for both spinel particles and matte droplets with a size of 10 and 75 microns and the results are shown in Figure 7.

The residence time of the slag in the furnace is reported by Lonmin to be roughly 16 hours, which is shown by the solid line on the plots in Figure 7. It is clear from Figure 7 that for 10 micron particles/droplets, the settling time is orders larger than the slag residence time, which should result in significant entrainment in the slag. For the

75 micron particles/droplets, the settling time for both matte and spinel is generally below the slag residence time, except for high silica addition, where the slag becomes more viscous. For the matte droplets, a low settling time is desired as any matte entrained in the slag results in a decrease in matte and PGM recovery. For the spinel particles the opposite is true, as a fast settling time will result in spinel accumulation between the matte and slag layers, the so-called 'mushy layer'. The formation of this layer between the matte and slag often results in the spinel phase being tapped out with the matte. This leads to a high chrome content in the matte, which causes problems in the highly oxidising and relatively low temperature environment encountered in the converting process.

From Equation [11] and Figure 7, it is clear that terminal settling velocity and therefore the settling time is highly dependent on the particle/droplet diameter. The matte droplets will, however, coalesce due to the mixing in the slag caused by the circulatory flow of the slag layer. Thus good mixing in the furnace is crucial as it will decrease matte entrainment in the slag. Good mixing will also hinder the settling of the spinel particles as unlike the matte, they will not coalesce on contact with one another. As mentioned in the introduction, one of the reasons that electrode immersion control is preferred to resistance setpoint control is that it results in better mixing in the bath and will thus minimize matte entrainment in the slag and at the same time hinder the formation of the 'mushy layer' between the matte and slag.

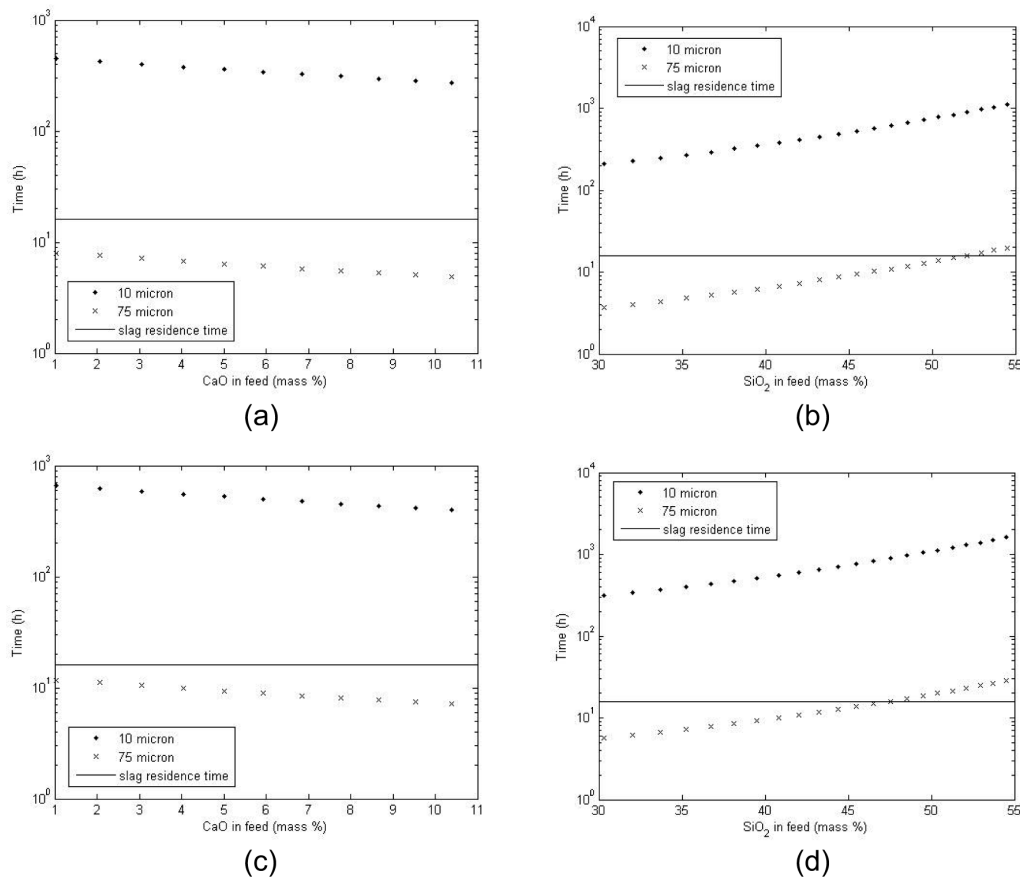


Figure 7. Settling time of matte droplets and spinel particles in matte as a function of the CaO and SiO₂ feeds to the furnace (T = 1 600°C).
 (a) Matte settling time vs CaO in feed, (b) Matte settling time vs SiO₂ in feed, (c) Spinel settling time vs CaO in feed,
 (d) Spinel settling time vs SiO₂ in feed

Ferrous vs ferric iron content in slag

An important variable used to calculate the electrical conductivity of the slag is the ratio of ferrous vs ferric iron in the slag. The FactSage simulations indicated that the iron in the slag was predominantly ferrous, with the lowest fraction of ferrous iron being roughly 0.93, but in the greater majority of the cases it was greater than 0.98. When the dip test was done on furnace No. 1, quenched slag samples were sent for analysis to determine the ratio of ferrous to ferric iron in the slag. The samples were taken over a period of 4 days and the results were relatively stable, with ferrous iron making up roughly 73% of the iron in the slag. This is much lower than the results obtained from FactSage and it was thought that the lack of any ferric iron inputs to the FactSage simulations was the cause of this. Ferric iron will mostly enter the furnace in the form of magnetite with its source being the converter slag that is recycled into the furnace.

In order to check this, some simulations were done in FactSage using the same typical feed composition used to assess the effects of the slag modifiers, except that Fe_3O_4 was added as an input. The ratio of oxidic iron entering as FeO or Fe_3O_4 was changed (while keeping the amount of oxidic iron constant) in order to see the effect of ferric iron input into the FactSage simulations. The results are shown in Figure 8 and it can be seen that there was very little effect and the iron in the slag is predominantly ferrous (> 99%) even if most of the oxidic iron is in the form of magnetite.

The effect of the carbon feed used in the FactSage simulations is also shown in Figure 8, as it was thought that perhaps this was a reason for the discrepancy between the FactSage results and the sample analyses, as the carbon was reducing the ferric iron into the ferrous state. While removing the carbon from the FactSage simulations does lower the amount of ferric iron in the slag, the difference is negligible. The reason for the discrepancy between the FactSage results and the furnace samples is therefore not known. One reason could be that the slag samples were perhaps not quenched sufficiently quickly and a fraction of the ferrous iron was therefore oxidized by air into the ferric state. This oxidation would occur rather quickly at the high slag temperatures found in the furnace.

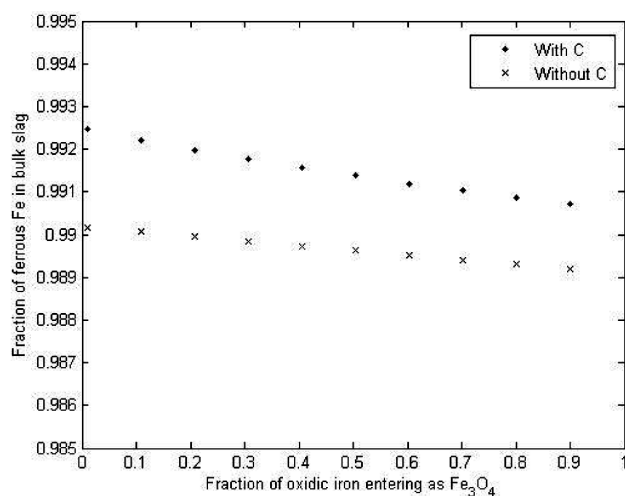


Figure 8. Ferrous iron in the slag as a function of oxidic iron input

Relationship between feed composition, resistance setpoint and electrode immersion

As discussed in section 2, the model is to be used to control the electrodes at a constant immersion in response to the disturbances in the feed. The main disturbance in the feed, with respect to its effect on the slag conductivity, is the oxidic iron content.

In Figure 9(a) the resistance setpoint, as calculated using the model, for varying FeO content in the feed is plotted for three different immersions. It is clear from the figure that if only the FeO in the feed is increased the slag becomes much more conductive, which results in the resistance setpoint being lowered by the model in order to ensure constant immersion. In Figure 9(b), a similar plot is shown for CaO. This plot shows a similar trend to that shown in Figure 9(a). Thus, for feed materials high in FeO, lime addition to the feed would be counterproductive as it would simply increase the conductivity of the slag even more. Figure 9(c) shows the effect of the ore blend (UG2 and Merensky) on the resistance setpoint. Interestingly, the changes to the resistance setpoint required are not nearly as dramatic as that shown in the other two figures. The reason for this is that while the UG2 ore contains roughly 20% more FeO, it also contains about 35% more SiO_2 than a typical Merensky ore. The higher silica content of the UG2 ore thus counteracts the increase in iron to a certain extent. Figure 9(d) shows the effect of blending the slag plant float material into the feed. This material is exceptionally high in FeO and has a FeO: SiO_2 ratio of close to 1. As such, it requires a relatively significant resistance setpoint to maintain a constant immersion. Thus it is the FeO: SiO_2 ratio in the feed material to the furnace that plays the major role in determining the conductivity of the slag, as alluded to in the introduction to this paper.

The model can also be used to determine how much silica should be added in order to decrease the conductivity of the slag and maintain the electrodes at the chosen constant immersion level for a specified resistance setpoint. This amount of SiO_2 that must be added is shown in Figure 10 for an increase in FeO content only (a), the UG2-Merensky blend ratio (b), and the slag plant float blend ratio (c), for a desired immersion of 50% and a resistance setpoint of 5 m Ω . It is clear from these figures that in order to maintain both a constant immersion and resistance setpoint, large amounts of silica may need to be added to the feed mixture. Obviously large additions of silica to the feed are somewhat unrealistic as it will decrease the smelting capacity of the furnace and also significantly increase the slag viscosity. However, the situation simulated in Figure 10 is somewhat unrealistic in that the furnace will never be operated at both constant immersion and resistance setpoint. Silica addition will only be considered if a situation is encountered where the resistance setpoint (which is to be the main manipulated variable) cannot be changed to the value necessary to ensure constant immersion without moving out of the P-V-I operating window of the furnace.

Slag conductivity—plant data

While the proposed feed sampling system is not as yet commissioned, the furnace slag is still sampled regularly and it is interesting to assess the changes in slag composition and its effect on the conductivity of the slag. In Table III the relevant statistics are shown for furnace No. 1 for the financial year 2007. The relative standard deviation (% RSD) shown in Table III is the standard deviation relative to the mean. Looking at these data it is clear that the variation is in the following order:

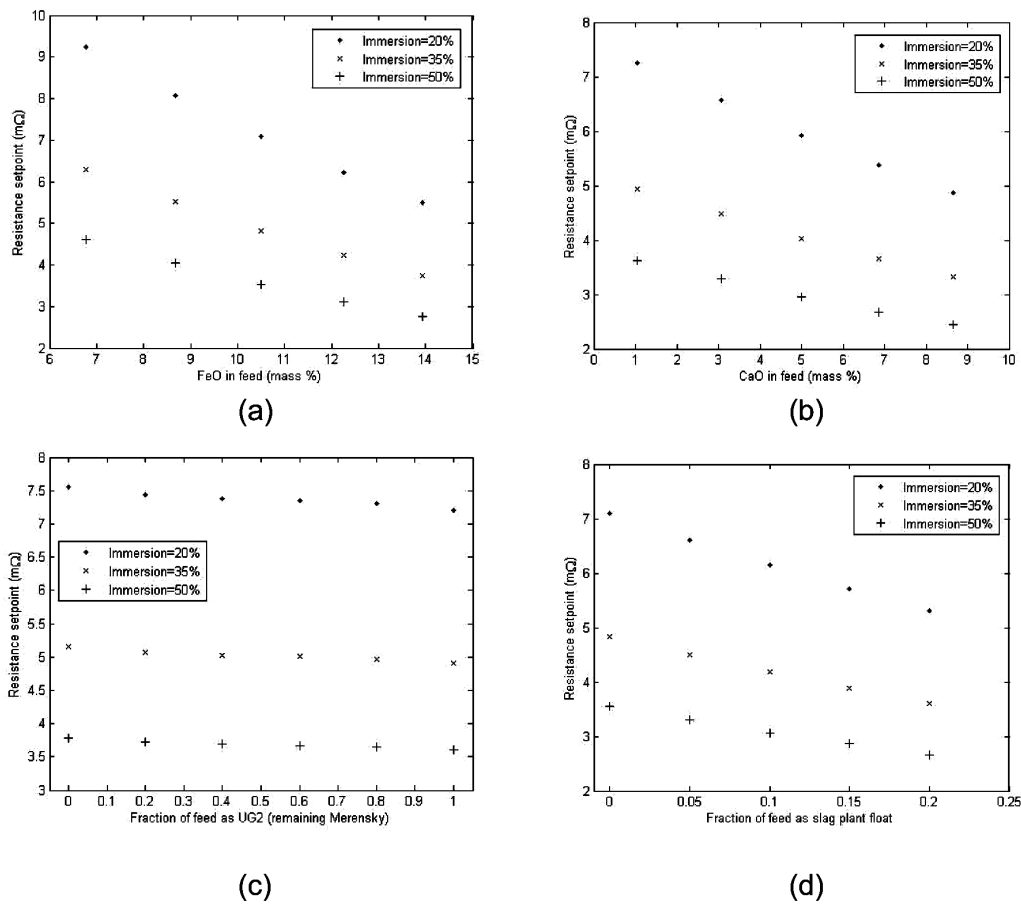


Figure 9. Effect of (a) FeO in feed, (b) CaO in feed, (c) UG2 fraction in ore blend and (d) slag plant float fraction in feed, on the resistance setpoint required for different immersions ($T = 1600^{\circ}\text{C}$)

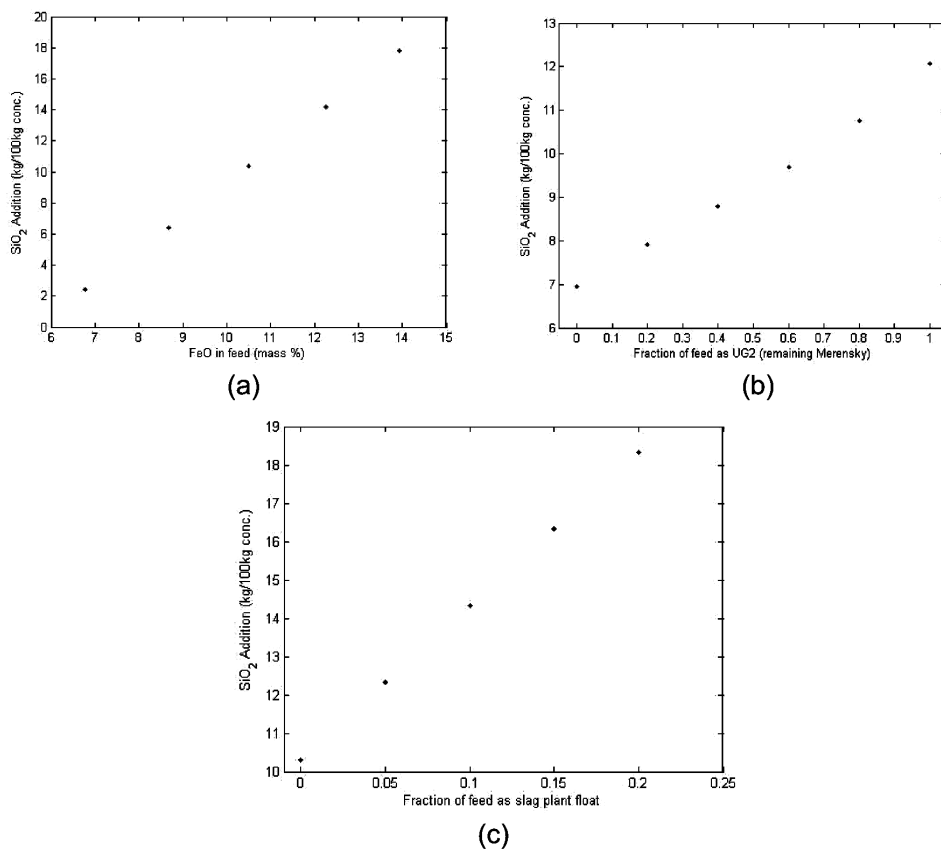


Figure 10. Amount of SiO_2 that must be added to the feed in order to ensure a constant electrode immersion of 50% at a resistance setpoint of 5 mΩ ($T = 1600^{\circ}\text{C}$). (a) Increase in FeO, (b) Fraction of feed as UG2, (c) Fraction of feed as slag plant float

Table III
Relevant slag composition statistics for furnace no. 1 for financial year 2007

	FeO (mole %)	Al ₂ O ₃ (mole %)	MgO (mole %)	CaO (mole %)	SiO ₂ (mole %)
Mean	12	3	30	9	46
St dev	1.8	0.27	1.5	2.9	1.85
% RSD	15	9	5	32	4

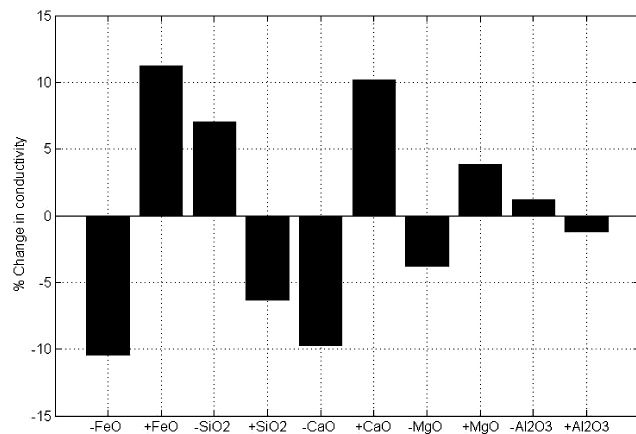


Figure 11. Sensitivity analysis for selected slag components at 1 600°C using the model of Hundermark¹ with perturbations equal to one standard deviation for each component

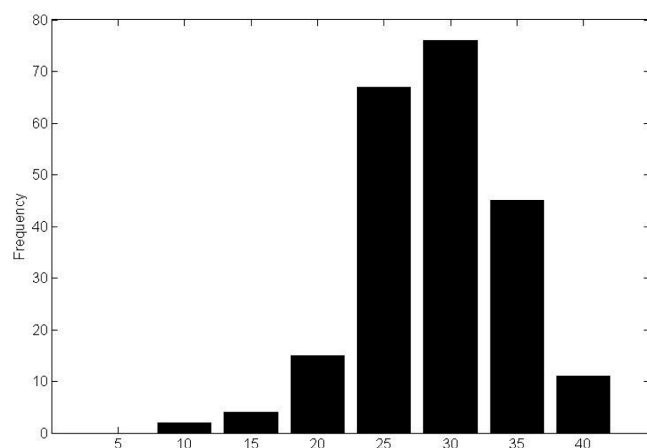


Figure 12. Histogram of required electrode immersion for furnace no. 1, financial year 2007

CaO > FeO > Al₂O₃ > MgO > SiO₂

The largest variation of CaO is purely due to the variable addition rate. For CaO in the concentrates (i.e. feed excluding lime addition), the %RSD is around 19% (vs. 32% in the slag). In Figure 11, a sensitivity analysis plot similar to that shown in Figure 4 is given where the average slag composition given in Table III is used. Each component composition is perturbed in the positive and negative direction by the standard deviation for the respective component, and the effect on the conductivity assessed. While the sensitivity analysis shown in Figure 4 gave an indication as to which variables have the greatest effect on conductivity in general, the plot shown in Figure 11 shows which components have the greatest effect on the smelter.

With regard to the historical slag composition, it is clear from Figure 11 that FeO has the greatest effect on the slag conductivity, followed by CaO, SiO₂ and MgO. As mentioned, the standard deviation of the CaO is largest as it is added independently as flux along with the concentrate. It is unclear how the amount of lime added to the furnace feed was determined on the smelter (as no thermodynamic model was available prior to this work), and from Figure 11 it is apparent that indiscriminate lime addition to the furnace could have a very large effect on the slag conductivity.

Using the 2007 financial year slag composition data, the conductivity of the slag for each day of operation was calculated with Equation [4], assuming a slag temperature of 1 600°C and that all of the iron in the slag is in the ferrous state. This was then used in conjunction with Equation [2], the calibrated furnace geometric factor model, an assumed resistance setpoint of 4 mΩ and a slag depth of 1 m to calculate the required electrode immersion (%). The results are presented as a histogram shown in Figure 12.

While the immersion data shown in Figure 12 are not the actual plant immersion data, the information is still valuable as it gives an indication of the electrode immersion distribution that is achieved when running the furnace using the electrode immersion as the manipulated variable, instead of the resistance setpoint as proposed in this paper.

The distribution shows that in the majority of cases the immersion was, in fact, in the region that is considered best for mixing in the slag ($\pm 30\%$). This implies that running the furnace using the resistance setpoint as a manipulated variable as proposed in this paper should not be too problematic as the furnace is already operating in that region. As such, minor adjustments to the resistance setpoint, and in worse cases, possible small additions of slag modifiers, should allow for constant electrode immersion while still operating the furnace within the required P-V-I envelope.

Conclusions

The addition of a more advanced feed sampling system for the Lonmin No. 1 circular furnace, and the subsequent information regarding the split between oxidic and sulphidic iron entering the furnace, has made it possible to use thermodynamic models to predict the slag chemistry using thermodynamic models. This, combined with recently developed models for slag conductivity specifically for PGM smelting, and a furnace geometric factor model calibrated on the No. 1 furnace, make it possible to implement immersion control on the furnace, where the aim is to keep a constant immersion by manipulating the resistance setpoint.

The thermodynamic model was created keeping in mind that it would need to be hard coded into a control system. For this reason, minimisation algorithms needed to be avoided. This was overcome by generating a large database using FactSage and then using these data to train neural networks. The neural networks were found to model the data exceptionally well, with the lowest R^2 value being 98.42%.

The FactSage results predicted that the majority of the iron in the slag was in the ferrous state (> 0.98 in most cases). These values did not correspond to slag samples taken on the smelter, where the fraction of the iron in the ferrous state was roughly 0.73. This was thought to be due to the lack of any ferric iron feeds to the FactSage simulations but on closer analysis this was found not to be the case. As such it was concluded that the main reason for this discrepancy could be due to the fact that the samples taken from the furnace were not quenched quickly enough.

When some scenarios were run using the full model it was found that while lime addition was favourable due to its effect on the slag viscosity, it also increased the

conductivity of the slag and decreased the solubility of chrome in the liquid portion of the slag, both of which are undesirable effects.

The high levels of FeO in the UG2 ore (compared to that in concentrates sourced from the Merensky ore) was found not to have a great effect on the conductivity of the slag, as the UG2 materials also contain significantly more silica than the Merensky material, which counteracts the effect of the FeO on the slag conductivity. The slag plant float material was found to be much more problematic, as it is very high in FeO and relatively low in silica, which results in exceptionally conductive slags. The amount of this material blended into the feed to the furnace must therefore be monitored and minor silica addition to the furnace feed may be required when large amounts of the slag plant float material is fed to the furnace.

Acknowledgements

The authors would like to thank Mr Bennie Du Toit, Mr Philip Nel, Mr Aubrey Larkins and Ms Wendy Malgas from Lonmin for their contribution to this work.

Nomenclature

Arabic symbols

a	Constant parameter in Einstein-Roscoe equation
D	Diameter (m)
D_e	Electrode diameter (cm)
f	Mass fraction of solids in slag
Fe^{2+}	Fraction of ferrous ions
Fe^{3+}	Fraction of ferric ions
f_g	Furnace geometric factor (cm^{-1})
g	Acceleration due to gravity (m/s^2)
H_s	Slag height (cm)
I	Current (A)
k	Cell constant
n	Constant parameter in Einstein-Roscoe equation
P	Power (MW)
PF	Power factor
R	Electrode resistance ($m\Omega$)
T	Slag temperature (K)
V_T	Terminal settling velocity (m/s)
X	Mol fraction
X_s	Electrode penetration into slag (cm)

Greek symbols

η	Viscosity of the solid containing slag (Pa·s)
η_0	Viscosity of the liquid portion of the slag (Pa·s)
ρ	Slag density (g/cm^3)
ρ_{fluid}	Density of liquid media in which particle/droplet is settling (kg/m^3)



Greg Georgalli

Researcher
Stellenbosch University

Completed my BEng(Chem) in 1999 and my MSc(Eng) in 2002, both from Stellenbosch University. From September 2002 until

February 2007 I worked as a researcher at the Technical University of Delft. In April 2007 I started as a researcher in pyrometallurgy at Stellenbosch University, where I am currently employed.



Jacques Eksteen

Consulting Metallurgist, Lonmin

He has graduated with all degrees from the University of Stellenbosch. He has worked for three years in process metallurgy and new product industrialisation at the Atomic Energy Corporation (now NECSA), before joining the University of Stellenbosch in 1998 to lecture and research in Extractive Metallurgy and Mineral Processing. During his 9 year academic career he has published over 60 peer reviewed journal publications and refereed conference proceedings, and delivered 22 postgraduate students at MSc and PhD level.

He has joined Lonmin as Consulting Metallurgist on Smelting and Refining in 2007 and is currently working within the Process Division Technical Support department.

$\rho_{particle}$ Density of particle/droplet settling in slag (kg/m^3)
 σ Slag conductivity ($(\Omega\cdot cm)^{-1}$)

References

- HUNDERMARK, R. The electrical conductivity of melter type slags. Master's thesis, University of Cape Town, 2003.
- GEORGALLI, G.A., EKSTEEN, J.J. and REUTER, M.A. An integrated thermochemical-systems approach to the prediction of matte composition dynamics in an Ausmelt® nickel-copper matte converter. *Minerals Engineering*, vol. 15, 2002. pp. 909–917.
- EKSTEEN, J.J., GEORGALLI, G.A. and REUTER, M.A. Online prediction of the actual melt chemistry in an Ausmelt converter using a thermodynamic - system identification hybrid modelling technique. In Proceedings of the Third International Sulphide Smelting Symposium, Seattle, February 2002. TMS. pp. 457–468.
- Lonmin Plc. Mineralogical and chemical analyses of the smelter primary and secondary concentrate streams and recycle streams. Personal communication.
- Lonmin Plc. Lonmin dry concentrate delivery plan. Personal communication, 2008.
- JIAO, Q. and THEMELIS, N.J. Correlation of geometric factor for slag resistance furnaces. *Metallurgical and Materials Transactions B*, vol. 22B 1991. pp. 182–192.
- SHENG, Y.Y., IRONS, G.A. and TISDALE, D.G. Transport phenomena in electric smelting of nickel matte: Part I. Electric potential distribution. *Metallurgical and Materials Transactions B*, vol. 29B 1998. pp. 77–83.
- UTIGARD, T.A. and WARCZOK, A. Density and viscosity of copper/nickel sulphide smelting and converting slags. In Proceedings of COPPER 95 - COBRE 95 International Conference, vol. IV - Pyrometallurgy of Copper, 1995. pp. 423–437.
- ZHANG, L., JAHANSHAHI, S., SUN, S., LIM, M., BOURKE, B., WRIGHT, S. and SOMERVILLE, M. Development and applications of models for pyrometallurgical processes. *Materials Forum*, vol. 25, 2001. pp. 136–153.
- DE NEVERS, N. *Fluid mechanics for chemical engineers*. McGraw-Hill, 2nd edition, 1991.